

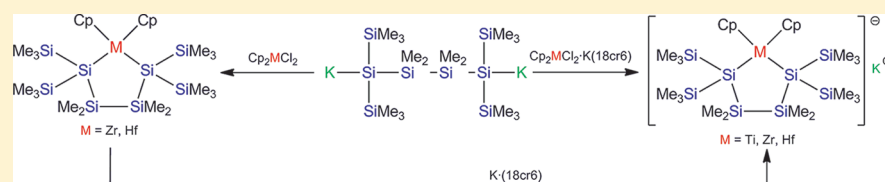
Synthesis of Oligosilanyl Compounds of Group 4 Metallocenes with the Oxidation State +3

Henning Arp,[†] Michaela Zirngast,[†] Christoph Marschner,^{*,†} Judith Baumgartner,^{*,†} Kenneth Rasmussen,[‡] Patrick Zark,[§] and Thomas Müller^{*,§}

[†]Institut für Anorganische Chemie and [‡]Institut für Physikalische Chemie, Technische Universität Graz, Stremayrgasse 9, A-8010 Graz, Austria

[§]Institut für Reine und Angewandte Chemie, Carl von Ossietzky Universität Oldenburg, Carl-von-Ossietzky-Straße 9-11, D-26211 Oldenburg, Federal Republic of Germany

S Supporting Information



ABSTRACT: Recently, we showed that titanocene silyls are much more stable with Ti in the oxidation state +3. The current study demonstrates that analogous Zr and Hf compounds can also be obtained by reaction of a suitable metalate precursor with an oligosilanyl dianion. As the obtained complexes formally possess a d^1 electron configuration, they were investigated using EPR spectroscopy. The corresponding spectra indicate that the compounds can be considered to also exhibit some cyclosilanyl radical anion character. In order to understand the strong preference of disilylated titan(IV)ocenes for reductive elimination, a theoretical study of the thermodynamics of these reactions was conducted, revealing that this behavior is essentially caused by the weak Si–Ti(IV) bond.

INTRODUCTION

Over the last few decades alkyl-substituted group 4 metallocenes have become a very well established class of compounds, for which numerous applications have been found.¹ Analogous compounds with higher group 14 substituents have received much less attention. However, silylated metallocenes are another interesting class of compounds which can serve as catalysts or catalyst precursors for a number of important chemical transformations. Prominent among these reactions is the dehydrogenative coupling polymerization of hydrosilanes,^{2–5} an important synthetic alternative to the Wurtz type coupling of chlorosilanes, which still is the most widely used method for the formation of Si–Si bonds in general and the synthesis of polysilanes⁶ in particular. The reaction was discovered by Harrod and co-workers as a process where PhSiH_3 reacts to give polyphenylsilane, $\text{H}(\text{PhSiH})_n\text{H}$, in the presence of Cp_2TiMe_2 .⁷ Harrod's initial mechanistic explanation involved the formation of the dinuclear Ti(III) complex $[\text{Cp}_2\text{TiSiH}_2\text{Ph}]_2$ as a source of the silylene PhSiH , which upon release could oligomerize to longer chains.^{8,9} Subsequently, Tilley and co-workers showed that the polymerization of phenylsilanes can also be catalyzed by zirconocenes and hafnocenes of the type $\text{CpCp}'\text{M}(\text{X})\text{H}$ ($\text{Cp} = \text{C}_5\text{H}_5$, $\text{Cp}' = \text{C}_5\text{H}_5$, C_5Me_5 ; $\text{M} = \text{Zr, Hf}$; $\text{X} = \text{Cl, Me}$) starting with catalyst precursors such as $\text{CpCp}'\text{M}(\text{X})\text{Si}(\text{SiMe}_3)_3$. For these systems, featuring the metal in the oxidation state +4, it was conclusively demonstrated that the

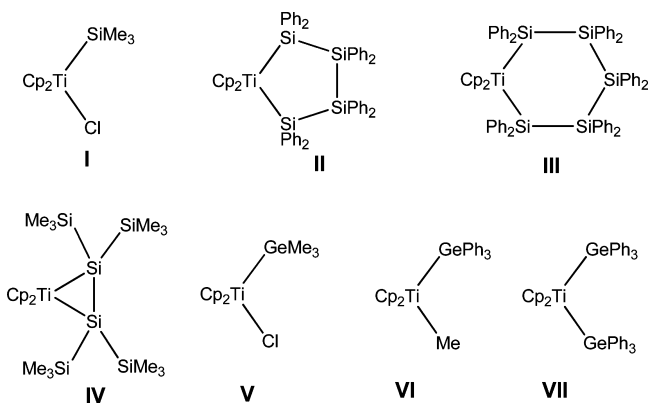
catalytic cycle consists of two σ -bond metathesis steps.^{2,10} While Harrod later expressed his belief that also in the titanium-catalyzed reaction “the key catalyst species is $\text{Cp}_2\text{Ti}(\text{H})\text{SiH}_2\text{R}$ ”,¹¹ it is interesting to note that still no examples of stoichiometric σ -bond metathesis reactions between silicon hydrides and bis(silyl)titanocenes or silylhydridotitanocenes are known. Even the syntheses of the disilylated titanocenes or $\text{CpCp}'\text{Ti}(\text{Cl})\text{Si}(\text{SiMe}_3)_3$ have never been reported.

A survey of known silylated titanocenes reveals that while there are a fair number of Ti(III) complexes^{8,12–16} and even some $\text{Ti}^{\text{II}}-\text{SiH}$ σ -complexes,^{17–19} less than a handful of examples of silylated titanocenes with Ti(IV) have been reported. Among these compounds $\text{Cp}_2\text{Ti}(\text{Cl})\text{SiMe}_3$ (**I**),²⁰ prepared by Rösch et al. utilizing the reaction of Cp_2TiCl_2 with $\text{Al}(\text{SiMe}_3)_3 \cdot \text{Et}_2\text{O}$, is well characterized with ^1H and ^{13}C NMR and IR spectra and a low-quality crystal structure ($R = 16\%$). The titanacyclosilanes $\text{Cp}_2\text{Ti}(\text{SiPh}_2)_n$ ($n = 4$ (**II**), 5 (**III**))^{21–23} were reported as products of the reaction of Cp_2TiCl_2 with $\text{Li}(\text{Ph}_2\text{Si})_n\text{Li}$. While for $\text{Cp}_2\text{Ti}(\text{SiPh}_2)_4$ ^{21,22} ^1H and ^{13}C NMR spectra in acetone were reported, the formation of $\text{Cp}_2\text{Ti}(\text{SiPh}_2)_5$ ^{23,24} was substantiated by multinuclear (including ^{29}Si) NMR²⁴ and a crystal structure analysis.²³ The reported synthesis of the silylene-bridged complex $[\text{Cp}_2\text{Ti}(\text{SiH}_2)]_2$ obtained by Weiss from the reaction of Cp_2TiCl_2 with

Received: April 12, 2012

Published: May 21, 2012

$\text{H}_3\text{SiK}^{25}$ was later questioned by Harrod and co-workers, who repeated the published procedure and obtained only $[\text{Cp}_2\text{Ti}(\text{SiH}_3)_2]_2$.²⁶ One further example of a well-characterized disilylated titanocene was reported by our group. The reaction of Cp_2TiCl_2 with $(\text{Me}_3\text{Si})_2\text{KSiSiK}(\text{SiMe}_3)_2$ was found to give a titanacylotrisilane (**IV**).²⁷ This compound, however, can be interpreted either as containing Ti(IV) with silyl groups or as Ti(II) with a disilene ligand.



For analogous germylated titanocenes with Ti(IV) the situation is quite similar. $\text{Cp}_2\text{Ti}(\text{Cl})\text{GeMe}_3$ (**V**) was prepared by Rösch in a manner analogous to that described for $\text{Cp}_2\text{Ti}(\text{Cl})\text{SiMe}_3$ utilizing $\text{Al}(\text{GeMe}_3)_3 \cdot \text{Et}_2\text{O}$.²⁰ The triphenylgermylated compound $\text{Cp}_2\text{Ti}(\text{Me})\text{GePh}_3$ (**VI**) was obtained by Harrod and co-workers from the reaction of Cp_2TiMe_2 with Ph_3GeH . Related studies from Razuvaev's group showed that $\text{Cp}_2\text{Ti}(\text{GePh}_3)_2$ (**VII**) and $\text{Cp}_2\text{Ti}(\text{Cl})\text{GePh}_3$ are relatively stable at room temperature, while $\text{Cp}_2\text{Ti}(\text{GeEt}_3)_2$ decomposes rapidly at room temperature to Et_6Ge_2 .^{29,30} They also reported reactions of digermylecadmium or digermylemercury with Cp_2TiCl_2 and Cp_2TiCl to give small amounts of germylated titanocenes.³¹

Our own attempts to react Cp_2TiCl_2 with $(\text{Me}_3\text{Si})_3\text{SiM}$ ($\text{M} = \text{K}, \text{Li}, \text{MgBr}, \text{MgSi}(\text{SiMe}_3)_3$) met with no success until

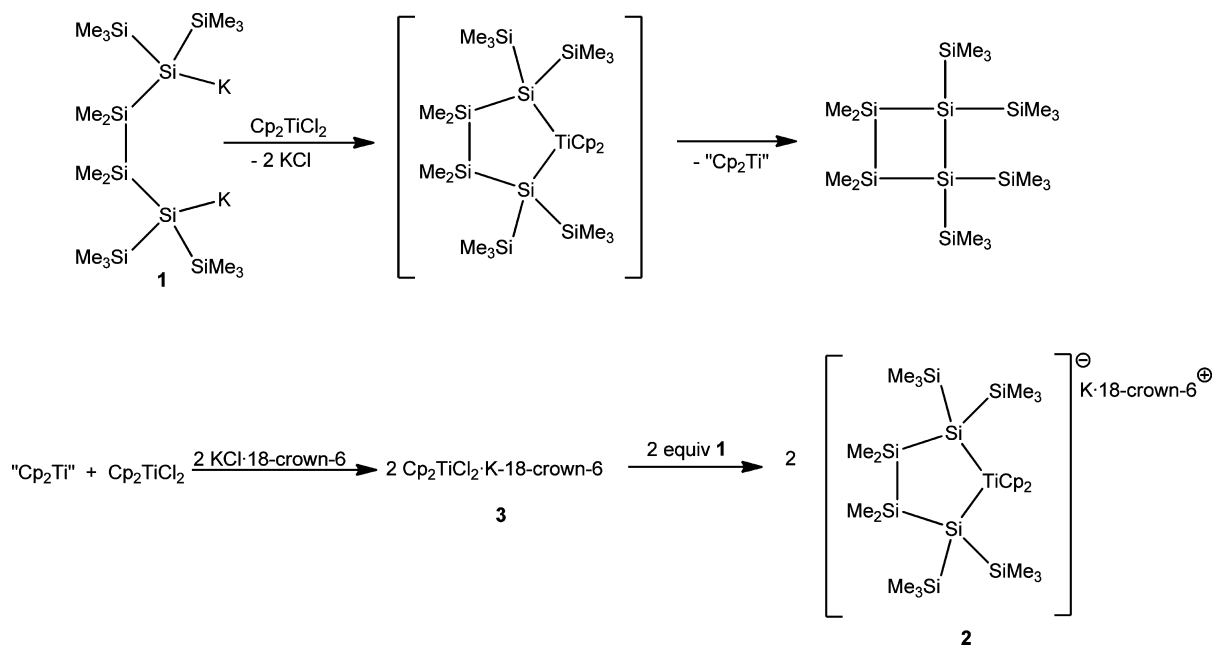
recently.³² While observation of the reaction of Cp_2TiCl_2 with $(\text{Me}_3\text{Si})_3\text{SiK} \cdot (18\text{-crown-6})$ by means of NMR spectroscopy did not indicate formation of any type of metalated tris(trimethylsilyl)silyl compound, it was possible to isolate another product: $\text{Cp}_2\text{TiCl}_2 \cdot \text{K}(18\text{-crown-6})$. The presence of this paramagnetic compound indicated the formation of paramagnetic, NMR-silent Ti(III) species in the reaction.³³ Continued attempts finally allowed the isolation of $\text{Cp}_2\text{Ti}(\text{Cl})\text{Si}(\text{SiMe}_3)_3 \cdot \text{K}(18\text{-crown-6})$, which was formed in a reaction that was not very clean. Changing from $(\text{Me}_3\text{Si})_3\text{SiK}$ to the dimetalated compound $\text{K}(\text{Me}_3\text{Si})_2\text{Si}(\text{Me}_2\text{Si})_2\text{Si}(\text{SiMe}_3)_2\text{K}$ (**1**)³⁴ led to a much cleaner course of reaction (Scheme 1). It was found that half of **1** was converted cleanly to 1,2-bis(trimethylsilyl)tetramethylcyclotetrasilane, which was presumably formed by reductive elimination of an initially formed titanacyclosilane. The concurrently formed titanocene "Cp₂Ti" likely underwent a comproportionation with Cp_2TiCl_2 to Cp_2TiCl , which in the presence of $\text{KCl} \cdot (18\text{-crown-6})$ reacted further to $\text{Cp}_2\text{TiCl}_2 \cdot \text{K}(18\text{-crown-6})$ (**3**).³² The latter could then react with the remaining **1** to give the final product, a titanacyclosilane (**2**) with titanium in the oxidation state +3.³²

The current study deals with further investigations concerning this reaction and, in particular, with the question whether this chemistry is also possible for the heavier metals of group 4.

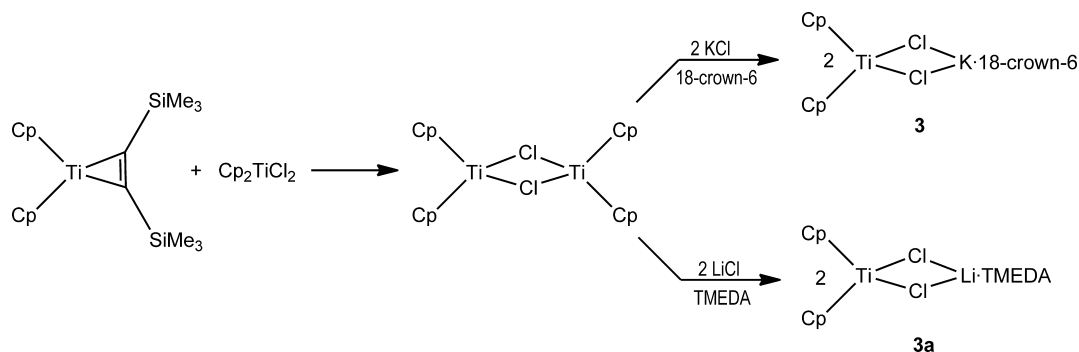
RESULTS AND DISCUSSION

Synthesis. Dichlorinated Metalates. Knowing that Ti(III) was involved in the reaction of Cp_2TiCl_2 with silyl anions, we set out to use another titanocene precursor to avoid wasting the metalated oligosilanes as reducing agents. While several methods for the synthesis of Cp_2TiCl and related complexes with reducing metals (such as Zn, Al, and Mn) are known,^{35,36} we thought to use comproportionation chemistry to obtain the $\text{Cp}_2\text{Ti}^{\text{III}}$ species in a way similar to that outlined above. Thus, the well-known "Cp₂Ti"³⁷ source $\text{Cp}_2\text{Ti}(\text{btmsa})$ ³⁸ was reacted with Cp_2TiCl_2 (Scheme 2). This reaction turned out to be a valuable source of "salt free" $(\text{Cp}_2\text{TiCl})_2$. The dinuclear

Scheme 1

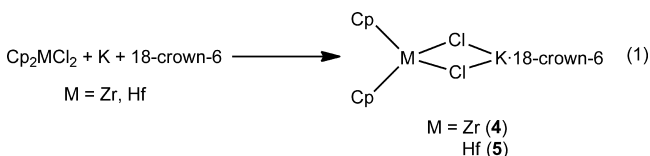


Scheme 2



$(\text{Cp}_2\text{TiCl})_2$ can further be converted to a mononuclear compound by reaction either with $\text{KCl}\cdot(18\text{-crown-6})$ or with LiCl in the presence of *tmeda* to obtain the respective base adducts of Cp_2TiCl with KCl (**3**) or LiCl (**3a**) (Scheme 2). This way the required precursors could be obtained without wasting oligosilane precursors, in a satisfying quantitative yield over two steps.

Reaction of **1** with Cp_2ZrCl_2 and Cp_2HfCl_2 was reported to lead to the formation of the respective metallacyclosilanes with the metals in the oxidation state +4, without any sign of reductive elimination.^{34,39} Therefore, attempts directed to the preparation of zirconium and hafnium analogues of **2** required metal salts of zirconocene and hafnocene in the oxidation state +3. The synthesis of the respective $\text{K}[\text{Cp}_2\text{ZrCl}_2]\cdot(18\text{-crown-6})$ (**4**) and $\text{K}[\text{Cp}_2\text{HfCl}_2]\cdot(18\text{-crown-6})$ (**5**) was thus accomplished in an even more straightforward fashion by reduction of the respective metallocene dichlorides with potassium in the presence of 18-crown-6 (eq 1).



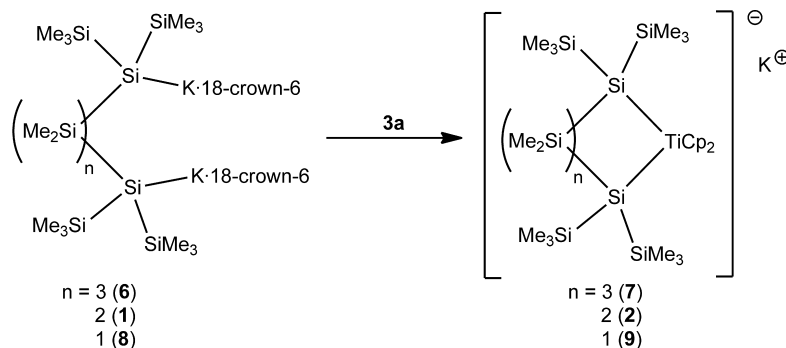
Disilylated Metalates. As anticipated, reactions of titanates **3** and **3a** with the dianion **1** led to the formation of the titanacyclopentasilane **2** in a cleaner way. Using **3a**, reactions with the respective 1,5-dipotassiopentasilane **6** and 1,3-dipotassiopentasilane **8** were also carried out. From the reaction of **3a** with **6** the expected anionic titanacyclohexasilane **7** could be obtained. The same anion could already be isolated from the reaction of **6** with Cp_2TiCl_2 .³² However, reaction of **6** with

Cp_2TiCl_2 gave the anionic part of **7** along with the complex counterion $[(\text{K}\cdot(18\text{-crown-6}))_2\text{Cp}]^+$, indicating a reaction course more complex than was anticipated, involving abstraction of a cyclopentadienide. The use of **3a** instead of Cp_2TiCl_2 provides a way to **7** with the simpler counterion $[(\text{K}\cdot(18\text{-crown-6}))\cdot 2\text{THF}]^+$ (Figure S1, Supporting Information).

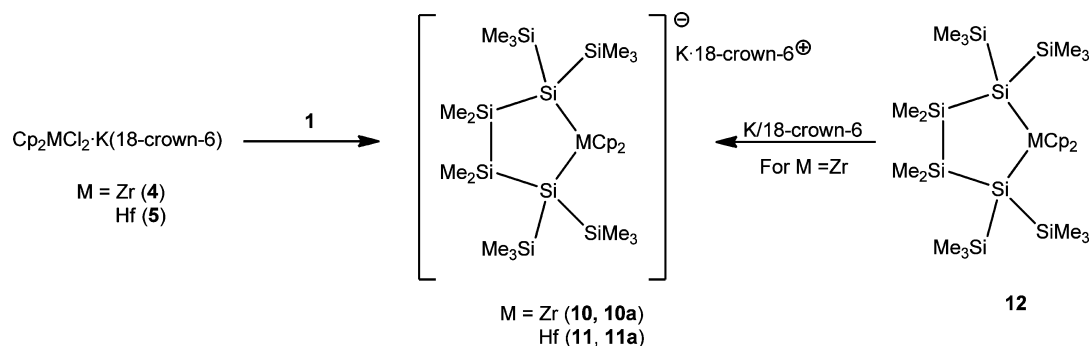
Disilanide **6** can be regarded as an elongated version of **1**, and in the same way **8** might be seen as the analogously shortened congener of **1**. As expected, the reaction of **8** with **3a** gave a complex anion comprised of a titanacyclopentasilane ring (**9**) (Scheme 3). In this case, however, single-crystal structure analysis showed that the counterion consists again of the complex $[(\text{K}\cdot(18\text{-crown-6}))_2\text{Cp}]^+$.

While the formation of **2**, **9**, and **7** utilizing **3a** proceeded in an expected way,³² it was also interesting to test whether the same reaction could also be accomplished for the analogous zirconium and hafnium cases. Therefore, the reactions of **1** with **4** and **5**, respectively, were carried out and found to proceed much in the same way as was observed for the titanium case (Scheme 4). This was striking, as the obtained products **10** and **11** contained the same metallacyclopentasilane unit with a d^1 electron configuration that were previously obtained as d^0 fragments.^{34,39} As it was possible to analyze the solid-state structures of all four compounds, a structural comparison allows some interesting conclusions about the relationship between geometry and electronic state (*vide infra*).

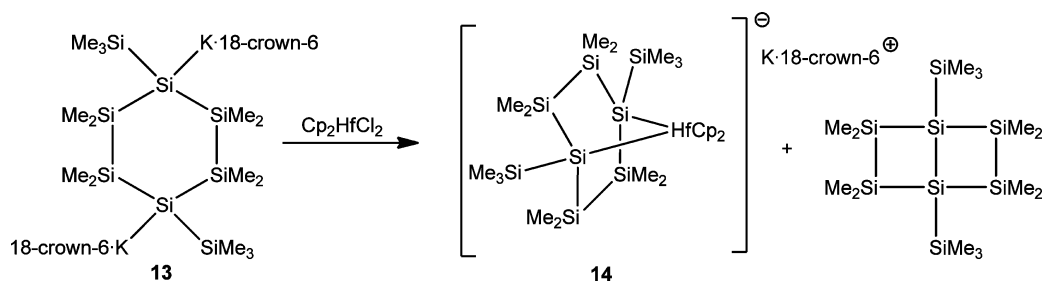
The subsequently arising question of whether the d^1 complex could be obtained also by direct reduction of the neutral metallacyclosilane was addressed by the reaction of the respective zirconacyclopentasilane **12** with 1 equiv of potassium in the presence of crown ether. It was found that this reaction yielded the d^1 complex directly (Scheme 4). However, while

Scheme 3. Formation of **2**, **7**, and **9**

Scheme 4



Scheme 5



crystal structure analysis of the resulting compound (**10a**) confirmed the identity of the expected d^1 zirconacyclopentasilane, it also featured the complex counterion $[(\text{K} \cdot (18\text{-crown-6}))_2\text{Cp}]^+$, which clearly indicates additional chemistry with cyclopentadienide acting as a leaving group, thus providing the possibility for the formation of $[(\text{K} \cdot (18\text{-crown-6}))_2\text{Cp}]^+$.

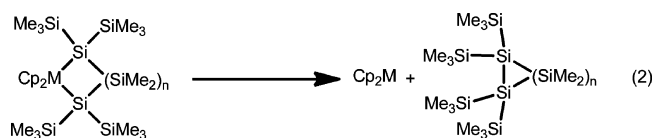
The successful preparation of the d^1 complexes of zirconacyclopentasilanes **10** and **11** and the strange behavior of the titanocenes forced us to revisit some chemistry that we found rather puzzling some years ago. While we found clean conversion of **1**, 1,4-dipotassiotetrasilane **1** with Cp_2ZrCl_2 and Cp_2HfCl_2 ,^{34,39} attempts to achieve the same conversion with the respective 1,4-dipotassicyclohexasilane **13**⁴⁰ with Cp_2ZrCl_2 and Cp_2HfCl_2 did not give any indication of the formation of the expected bicyclic metal-bridged compounds. Considering the course of the reaction of **1** with Cp_2TiCl_2 ³² and the fact that our judgment of the reactions was based primarily on NMR spectroscopic analysis, it seemed reasonable to reinvestigate the reaction of **13** with Cp_2HfCl_2 . Again, NMR spectroscopic observation gave no indication for the formation of the respective disilylated metalocene but provided evidence for the decomposition of this compound by reductive elimination, which gives the respective coupled cyclosilane that is already known.⁴⁰ However, crystallographic analysis revealed that the disilylated metalocene **14** was formed with the metal being in the oxidation state +3 (Scheme 5). A similar course of reaction had already been found for the titanocene case.³²

A simple explanation as to why it is possible to prepare some disilylated zirconocenes and hafnocenes with the metal in the oxidation state +4, while others that are seemingly very similar cannot be formed, is difficult to give. The question certainly seems to be related to the equally puzzling behavior of silylated titanocenes. It seems reasonable to assume that in the reaction of two silyl anions with Cp_2MCl_2 the expected disilylated metalocenes form initially but then undergo reductive elimination as the first step of the sequence, concluding with the formation of disilylated metalocenes in the oxidation state

+3. This leads directly to the question of why certain reductive elimination processes are more facile than others.

Computational Study. To understand the outlined unexpected reductive elimination behavior of disilylated titanocenes, we set out to conduct a computational study of these compounds and their zirconocene and hafnocene counterparts at the density functional MPW1PW91/SDD (Ti, Zr, Hf) and 6-311G(d,p) (H, C, Si) level of theory.^{41,42}

In order to obtain some initial insights, the thermodynamics involved in the reaction depicted in eq 2 were studied. In this



reaction the facility of reductive cyclosilane elimination from cyclic disilylated metallocene(IV) compounds is investigated as a function of metal and different ring size. The results of the calculations given in Table 1 correlate qualitatively with the observed experimental situation. While the reductive elimination of a disilene from the formal metallacyclopentasilane is endothermic (only slightly though for the Ti case) for all three

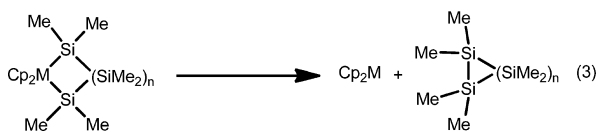
Table 1. Calculated Free Enthalpy Differences at 298.15 K, ΔG^{298} (kJ mol^{-1}), for the Reductive Elimination Reactions of Metallasilacycles with Concurrent Formation of Cyclosilanes According to Eq 2

elimination product	$n = 0$	$n = 1$	$n = 2$	$n = 3$
	disilene	cyclotrisilane	cyclotetrasilane	cyclopentasilane
metallacycle	three-membered	four-membered	five-membered	six-membered
Ti	3	-42	-121	-176
Zr	154	135	50	8
Hf	172	160	78	37

metals, the elimination is strongly favored for all other ring sizes of titanacyclosilanes and it is more favorable for large ring sizes. This calculated trend for the ease of the reductive elimination process from titanacyclosilanes follows the experimental observation. That is, we were able to synthesize and isolate a titanacyclotrisilane²⁷ but no larger titanacycles. For the zircona- and hafnacyclosilanes the same trend is found: the thermodynamic stability decreases with increasing ring size of the metallacycles. However, the situation is more delicate, as in all investigated cases the reductive elimination is predicted to be endothermic. In the experiment, however, reductive elimination is not an isolated process but is followed by subsequent reactions; therefore, the trend visible through the data summarized in Table 1 provides a rationalization of the experimental facts that the respective metallacyclotetrasilanes and -pentasilanes are stable while the metalocyclohexasilanes undergo reductive elimination.

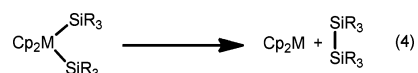
While the study of the reaction of eq 2 reflects the real systems qualitatively well, it does not provide an intuitive explanation. For this reason it was decided to vary the parameters of the system in order to obtain further insight.

The first variation applied was the replacement of the trimethylsilyl groups at the positions β to the metals by methyl groups (eq 3). The calculated free enthalpies ΔG^{298} according



to these reactions are given in Table 2. In principle the picture is the same as was found for eq 2, but all results are shifted to more endothermic values. For this system also the three- and four-membered titanacyclosilanes are predicted to be stable and reductive elimination becomes only a feasible process for five-membered and larger rings. For the heavier metals zirconium and hafnium six-membered rings should be stable. Although no calculations were carried out for phenyl substituents at the silicon atoms in α positions, the stability of this substitution pattern might be even higher, given the fact that a titanooctaphenylcyclopentasilane^{21,22} and even a titanadecaphenylcyclohexasilane are known.^{23,24} The trend outlined here also provides an explanation for the fact that $\text{Cp}_2\text{Ti}(\text{Cl})\text{SiMe}_3$ was found to be a stable compound while the synthesis of the analogous tris(trimethylsilyl)silyltitanocene chloride failed.³²

In order to eliminate the potential influence of ring strain of the formed cyclosilane the reductive elimination of two silyl substituents to give a disilane was studied computationally for comparison (eq 4). The steric requirements and the silylation degree of the silyl substituents were varied from trimethylsilyl to tris(trimethylsilyl)silyl, and the results of the calculations are



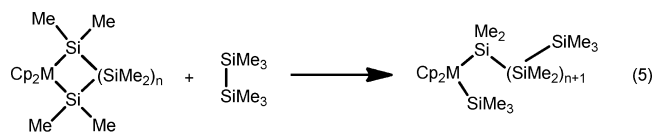
shown in Table 3. All disilylated titanocenes(IV) were found to be prone to facile reductive elimination. For zirconium and

Table 3. Calculated Free Enthalpy Differences at 298.15 K, ΔG^{298} (kJ mol^{-1}), for the Reductive Elimination Reactions of Disilylated Group 4 Metallocenes with Concurrent Formation of Disilanes According to Eq 4

M	R_3			
	Me_3	$(\text{SiMe}_3)_2\text{H}$	$(\text{SiMe}_3)_2\text{SiMe}_2\text{H}$	$(\text{SiMe}_3)_3$
Ti	-118	-130	-150	-155
Zr	+33	+46	+40	+26
Hf	+62	+73	+66	+53

even more for hafnium no energetically favorable eliminations were detected. This result clearly identifies the inherent weakness of the Ti(IV)–Si linkage as one of the major factors that determines the instability of silyltitanocenes(IV) and is further supported by the calculated mean bond dissociation energy, D_e , of the metal–silicon bond in $\text{Cp}_2\text{M}^{\text{IV}}(\text{SiMe}_3)_2$, which increases significantly with increasing atomic number of the metal ($M = \text{Ti}$, $D_e = 136 \text{ kJ mol}^{-1}$; $M = \text{Zr}$, $D_e = 206 \text{ kJ mol}^{-1}$; $M = \text{Hf}$, $D_e = 223 \text{ kJ mol}^{-1}$).⁴² Less clear is the trend revealed by the calculation upon α -silylation. For titanium a higher silylation degree was found again to correspond with a more favored elimination. For zirconium and hafnium, however, the stability of the metal–silicon bond does not decrease monotonically with increasing silylation degree, which seems to suggest that a higher silylation degree stabilizes the bond but becomes detrimental once steric interactions between the silyl groups or between the silyl and Cp ligands arise. For the disilylated metallocenes ($M = \text{Zr}, \text{Hf}$) this situation occurs for (trisilyl)silyl substituents.

As the results of this reaction (eq 4, Table 3) are clearly different from those of the metallacycle reductive eliminations (eqs 2 and 3, Tables 1 and 2), a profound influence of ring strain can be assumed. However, as in the actual reaction both the starting material and the product are cyclic in nature, the thermodynamics of the isodesmic reaction⁴³ depicted in eq 5



were studied in order to assess the influence of ring strain of the metallacycle (Table 4). The results indicate that only the three-membered zircona- and hafnacycles are somewhat strained and,

Table 2. Calculated Free Enthalpy Differences at 298.15 K, ΔG^{298} (kJ mol^{-1}), for the Reductive Elimination Reactions of Metallacycles with Methyl Substituents at the α -Silicon Atoms and with Concurrent Formation of Cyclosilanes According to Eq 3

elimination product	$n = 0$	$n = 1$	$n = 2$	$n = 3$	$n = 4$
	disilane	cyclotrisilane	cyclotetrasilane	cyclopentasilane	cyclohexasilane
metallacycle	three-membered	four-membered	five-membered	six-membered	seven-membered
Ti	82	15	-62	-108	-151
Zr	215	170	75	30	0
Hf	237	194	106	61	31

Table 4. Calculated Energies, ΔE (kJ mol⁻¹), for the Isodesmic Reactions (Eq 5) Which Determine the Ring Strain of the Metallacycles

metallacycle	$n = 0$	$n = 1$	$n = 2$	$n = 3$
	three-membered	four-membered	five-membered	six-membered
Ti	7	24	30	23
Zr	-14	22	14	15
Hf	-21	16	15	17

even more important, that there is no evident correlation among ring strain, metal, and ring size for cycles with more than three constituent atoms.

The fact that the results given in Table 3 substantially differ from those in Table 1 indicates that ring strain is effectively involved as a factor for the reductive elimination of metallacyclosilanes. However, when it is not the strain that is effective in the metallacycles (as can be concluded from the results given in Table 4), the strain of the cyclosilane products needs to be taken into consideration. This was attempted by studying the isodesmic reaction⁴³ outlined in eq 6, and the results are given in Table 5.

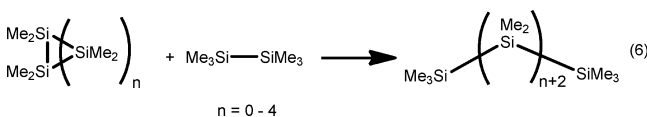


Table 5. Calculated Energies, ΔE (kJ mol⁻¹), for the Isodesmic Reactions (Eq 5) Which Determine the Ring Strain of the Polysilacycles (Me₂Si)_n ($n = 1-4$)

starting material	n	ΔE
tetramethyldisilene	0	-207
hexamethylcyclotrisilane	1	-134
octamethylcyclotetrasilane	2	-47
decamethylcyclopentasilane	3	-8
dodecamethylcyclohexasilane	4	3

While the calculations might not reproduce the actual system accurately because the additional steric interaction involved in the formation of the 1,1,2,2-tetrakis(trimethyl)disilanyl unit is not accounted for, it gives a good idea that five- and six-membered rings essentially experience no or only little ring strain.⁴⁴ This tells us that for the cases of the three-, four-, and five-membered metallacycles a ring strain component works against a facile reductive elimination to give cyclic products. The behavior of the respective zirconium and hafnium compounds is consistent with this.

EPR Spectroscopy. While the d¹ configuration of the studied complexes does not permit NMR spectroscopic investigations, it allows the use of EPR spectroscopy. Especially for the study of titanocene and to some extent zirconocene d¹ complexes this is a very established technique. In fact, there exists even a prior EPR study of radical anions of group 4 metallacyclohexasilanes, namely titana- and zirconadecaphenylcyclohexasilane,²⁴ which addressed the question of electron delocalization within the cyclosilane framework.

In the course of this study we investigated compounds **2**, **4**, **10**, and **11**. The dichlorinated metalate **4** exhibited a signal at $g = 1.970$ with the expected hyperfine coupling to ⁹¹Zr ($a(I =$

$5/2) \approx 27$ G), which is in excellent agreement with the values reported by Samuel et al. for [Cp₂ZrCl₂]⁻ ($g = 1.970$, $a(I = 5/2) \approx 29.7$ G).⁴⁵ In contrast to this, the EPR spectrum of **10** shows a slightly more complex signal with coupling also to the α -silicon atoms (Figure 1). The smaller value of the hyperfine

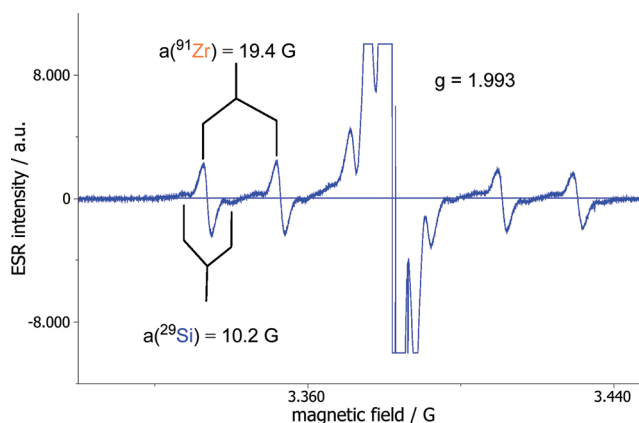


Figure 1. EPR spectrum of **10** at rt in C₆H₆.

splitting (hfs) constant to ⁹¹Zr, $a(I = 5/2) = 19.4$ G, indicates a delocalization of the electron between the metal and the attached silicon atoms. A hfs of 10.2 G to ²⁹Si can be compared to the value of 7.1 G measured for the coupling to trimethylsilyl groups in (Me₃Si)₃Si[•].⁴⁶ Due to the presence of ⁴⁷Ti ($I = 5/2$) and ⁴⁹Ti ($I = 7/2$), which both display a hfs of 8.8 G, the spectrum of **2** (Figure 2) is more complicated; still, the hfs to

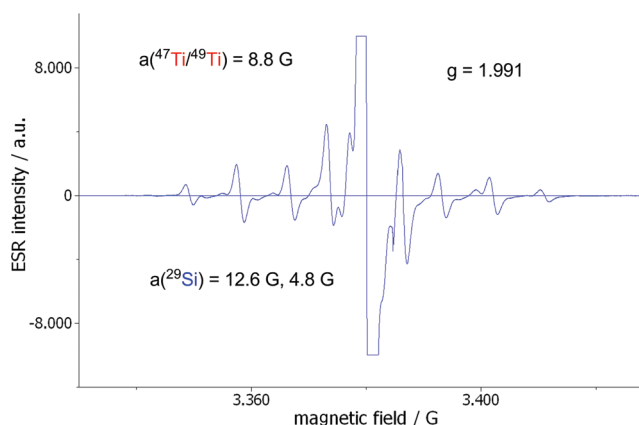


Figure 2. EPR spectrum of **2** at rt in C₆H₆.

the α -²⁹Si atoms is 12.6 G, of the same magnitude as observed for **10**. In addition, the simulation of the spectrum provides a hfs owing to another spin $1/2$ nucleus with the double natural abundance of silicon with a magnitude of 4.8 G. For reasons of symmetry as well of geometry, we assign this coupling to the SiMe₂ groups in β positions, which lie in the plane of the five-membered ring. In contrast to the well-resolved spectra of **2** and **10**, the spectrum of **11** displayed an ESR signal at a g value of 1.986 with very broad lines, likely indicating unresolved hyperfine coupling to ¹⁷⁷Hf and ¹⁷⁹Hf as well as to ²⁹Si.

Structural Analysis. Compounds **3a**, **4**, **7**, **9**, **10**, **11**, **11a**, and **14** were subjected to single-crystal structure analysis (Table 6). The quality of the structures of compounds **7**, **9**, and **11a** was not sufficient to allow a detailed structural discussion but nevertheless unambiguously proved the bond connectivity of

Table 6. Crystallographic Data for Compounds 3a, 4, 10, 11, and 14

	3a	4	10	11	14
empirical formula	C ₁₆ H ₂₆ Cl ₂ LiN ₂ Ti	C ₂₂ H ₃₄ Cl ₂ KO ₆ Zr	C ₄₇ H ₉₈ KO _{7.5} Si ₈ Zr	C ₃₈ H ₈₂ HfKO ₆ Si ₈	C ₄₃ H ₈₄ HfKO ₆ Si ₈
M _w	372.13	595.71	1141.30	1077.35	1139.41
temp (K)	100(2)	100(2)	100(2)	100(2)	200(2)
size (mm)	0.44 × 0.32 × 0.24	0.30 × 0.26 × 0.12	0.38 × 0.29 × 0.19	0.38 × 0.24 × 0.24	0.32 × 0.30 × 0.20
cryst syst	tetragonal	monoclinic	monoclinic	triclinic	monoclinic
space group	P4 ₃ 2 ₁ 2	P2 ₁ /c	P2 ₁ /c	P $\bar{1}$	P2 ₁ /c
a (Å)	8.2533(2)	11.539(2)	22.150(4)	11.0602(2)	13.884(3)
b (Å)	8.2533(2)	11.888(2)	15.819(3)	13.291(3)	15.265(3)
c (Å)	27.378(6)	19.059(4)	18.277(4)	21.226(4)	27.786(6)
α (deg)	90	90	90	77.47(3)	90
β (deg)	90	95.56(3)	96.07(3)	81.03(3)	99.18(3)
γ (deg)	90	90	90	70.17(3)	90
V (Å ³)	1865(3)	2602(2)	6368(2)	2854(2)	5813(2)
Z	4	4	4	2	4
ρ _{calcd} (g cm ⁻³)	1.325	1.521	1.190	1.254	1.298
abs coeff (mm ⁻¹)	0.742	0.822	0.430	2.103	2.069
F(000)	780	1228	2450	1122	2372
θ range (deg)	2.58 < θ < 25.15	1.77 < θ < 26.37	1.58 < θ < 26.35	1.97 < θ < 26.33	1.48 < θ < 26.37
no. of collected/unique rflns	13 218/1668	13 467/5257	50 196/12 942	22 736/11 430	45 501/11 867
completeness to θ (%)	99.9	99.0	99.6	98.4	99.8
no. of data/restraints/params	1668/0/104	5257/0/308	12 942/0/649	11 430/0/503	11 867/0/547
goodness of fit on F ²	1.25	1.07	1.03	1.03	1.11
final R indices (I > 2σ(I))	R1 = 0.057, wR2 = 0.116	R1 = 0.051, wR2 = 0.103	R1 = 0.049, wR2 = 0.107	R1 = 0.065, wR2 = 0.121	R1 = 0.066, wR2 = 0.124
R indices (all data)	R1 = 0.060, wR2 = 0.117	R1 = 0.071, wR2 = 0.111	R1 = 0.068, wR2 = 0.1151	R1 = 0.088, wR2 = 0.129	R1 = 0.090, wR2 = 0.135
largest diff peak/hole (e/Å ³)	0.48/−0.32	0.74/−0.38	0.75/−0.57	2.37/−1.89	1.44/−1.48

the respective complexes. Molecular structures and crystallographic details of **7**, **9**, and **11a** are provided in the Supporting Information.

Dichlorotitanate **3a** crystallizes in the tetragonal space group P4₃2₁2. Its structure (Figure 3) is similar to that already reported for **3**.³² The titanium, chlorine, and lithium atoms

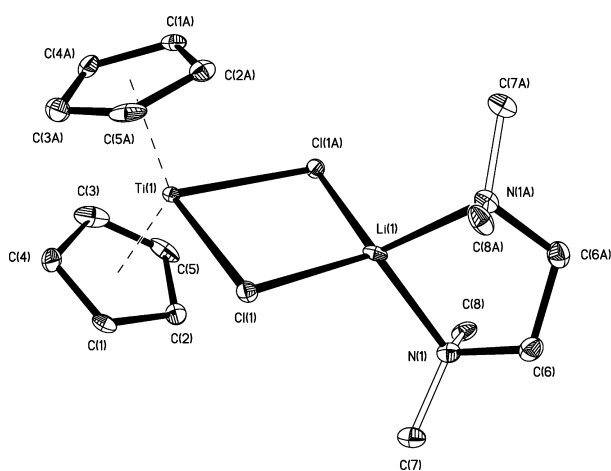


Figure 3. Crystal structure of **3a**. Thermal ellipsoids are represented at the 30% probability level, and hydrogen atoms have been omitted for clarity. Selected bond distances (Å) and angles (deg): Ti(1)–C(2) = 2.355(4), Ti(1)–Cl(1) = 2.5451(13), Li(1)–N(1) = 2.057(9), Li(1)–Cl(1) = 2.294(8); Cl(1A)–Ti(1)–Cl(1) = 86.02(6), N(1)–Li(1)–N(1A) = 89.5(5), N(1)–Li(1)–Cl(1) = 115.98(11), N(1A)–Li(1)–Cl(1) = 119.34(11).

form a planar four-membered ring with a tmeda molecule coordinating to lithium, thus extending its coordination number to 4. The length of the two equivalent Ti–Cl bonds is, at 2.54 Å, even slightly longer than that for **3**³² but comparable to that for [Cp₂TiCl]₂ (2.54–2.56 Å).⁴⁷ This is, however, considerably longer than what was found for Cp₂TiCl₂ (2.36 Å).⁴⁸ Also the decrease in bond angle from 94° for Cp₂TiCl₂⁴⁸ to 80° for [Cp₂TiCl]₂⁴⁷ is reflected in **3a** (86°).

The situation for compound **4**, which crystallizes in the monoclinic space group P2₁/c with some disorder in the crown ether affecting atoms O1 and C11 (Figure 4), is similar to that for **3**.³² In contrast to the lithium titanate **3a**, the potassium metalates **3** and **4** do not feature a planar arrangement of the four-membered ring K–Cl–M–Cl but show puckerings of 37 and 39°, respectively. Crystal structures of binuclear Cp₂Zr^{III}Cl species are quite rare.^{49–52} All known compounds of the type display Zr–Cl distances of 2.55–2.60 Å, which is consistent with the 2.58 Å found for **4**. This is again substantially longer than the Zr–Cl distance of 2.44 Å found for Cp₂ZrCl₂.⁵³

The structure analysis of compounds **10** and **11** is interesting, as in these cases a comparison of the same structural units with the metal in the oxidation state +4 is possible. Structural differences reflect therefore most likely the different oxidation states.

The zircona(III)cyclopentasilane **10** (Figure 5) crystallizes in the monoclinic space group P2₁/c, whereas the related hafna(III)cyclopentasilanes **11** and **11a** crystallize in the triclinic space group P $\bar{1}$. The asymmetric unit of **10** contains the halves of a potassium crown ether unit coordinated by two THF molecules.

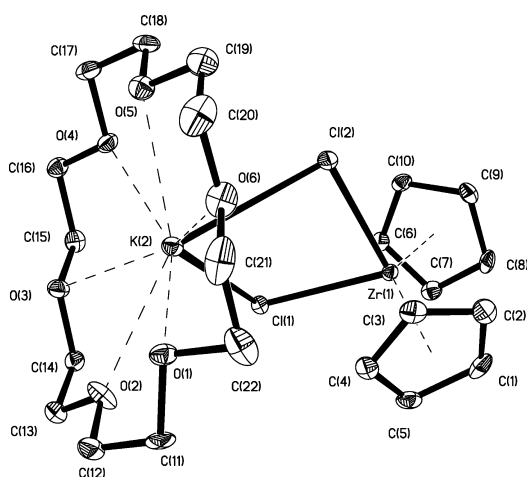


Figure 4. Crystal structure of **4**. Thermal ellipsoids are represented at the 30% probability level, and hydrogen atoms have been omitted for clarity. Selected bond distances (Å) and angles (deg): Zr(1)–Cl(1) = 2.5841(11), Zr(1)–Cl(2) = 2.5883(11), Cl(1)–K(2) = 3.1196(13), Cl(2)–K(2) = 3.2204(15); Cl(1)–Zr(1)–Cl(2) = 82.31(3), Zr(1)–Cl(1)–K(2) = 99.17(4), Zr(1)–Cl(2)–K(2) = 96.57(3), Cl(1)–K(2)–Cl(2) = 64.92(3), Cl(1)–K(2)–Zr(1) = 35.84(2), Cl(2)–K(2)–Zr(1) = 36.17(2).

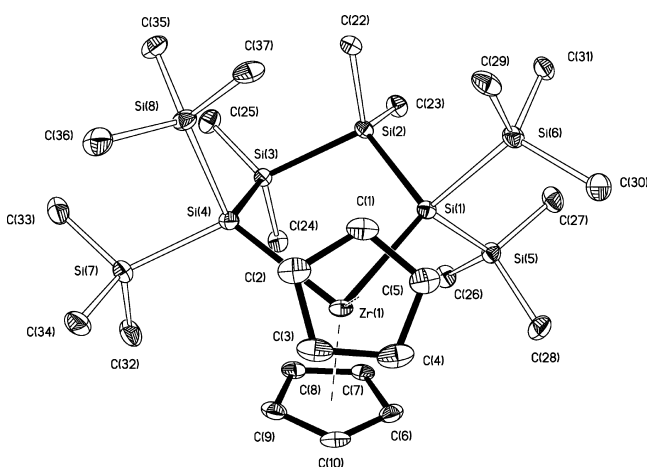


Figure 5. Crystal structure of **10** (the cationic part is omitted for reasons of clarity). Thermal ellipsoids are represented at the 30% probability level, and hydrogen atoms have been omitted for clarity. Selected bond distances (Å) and angles (deg): Zr(1)–C(1) = 2.487(3), Zr(1)–Si(4) = 2.8503(11), Zr(1)–Si(1) = 2.8950(10), Si(1)–Si(6) = 2.3626(11), Si(1)–Si(2) = 2.3674(13), Si(1)–Si(5) = 2.3705(11), Si(2)–Si(3) = 2.3329(12), Si(3)–Si(4) = 2.3642(11), Si(4)–Si(7) = 2.3627(12), Si(4)–Si(8) = 2.3825(11); Si(4)–Zr(1)–Si(1) = 85.65(3), Si(6)–Si(1)–Si(2) = 99.84(4), Si(6)–Si(1)–Si(5) = 98.07(4), Si(2)–Si(1)–Si(5) = 102.82(4), Si(3)–Si(2)–Si(1) = 104.05(4), Si(2)–Si(3)–Si(4) = 103.45(4), Si(7)–Si(4)–Si(3) = 103.32(4), Si(7)–Si(4)–Si(8) = 98.17(4), Si(3)–Si(4)–Si(8) = 105.80(4).

Similar to the discussed relationship between Cp_2TiCl_2 and **3**, the Si–Zr–Si bond angle of **10** of 85.7° is diminished by some 12° in comparison to the structure with Zr(IV). Also the Zr–Si bond lengths within the zirconacyclopentasilane ring are somewhat elongated (2.85/2.90 Å) in relation to the Zr(IV) compound (2.86/2.85 Å), but not to the same extent as observed for the Cp_2MCl cases. The zirconacyclopentasilane ring of **10** adopts a perfect envelope conformation with one of

the SiMe_2 units on the flap, whereas the Zr(IV) ring³⁹ shows a half-twisted conformation.

The crystals for the structures of **11** (Figure 6) and **11a** (Figure S3, Supporting Information) were grown in the same

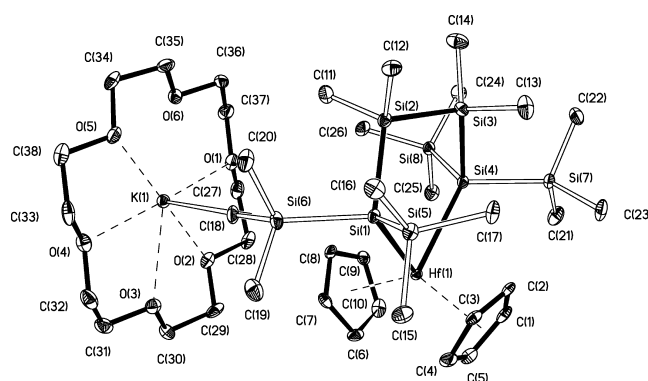


Figure 6. Crystal structure of **11**. Thermal ellipsoids are represented at the 30% probability level, and hydrogen atoms have been omitted for clarity. Selected bond distances (Å) and angles (deg): Hf(1)–Si(4) = 2.849(2), Hf(1)–Si(1) = 2.863(2), K(1)–C(23A) = 3.207(8), Si(1)–Si(2) = 2.366(3), Si(1)–Si(6) = 2.371(3), Si(1)–Si(5) = 2.380(3), Si(2)–Si(3) = 2.347(3), Si(3)–Si(4) = 2.372(3), Si(4)–Si(8) = 2.365(3), Si(4)–Si(7) = 2.378(3); Si(4)–Hf(1)–Si(1) = 89.10(6), Si(2)–Si(1)–Si(6) = 100.39(10), Si(2)–Si(1)–Si(5) = 103.30(10), Si(6)–Si(1)–Si(5) = 97.41(11), Si(3)–Si(2)–Si(1) = 108.10(11), Si(2)–Si(3)–Si(4) = 106.70(11), Si(8)–Si(4)–Si(3) = 102.95(10), Si(8)–Si(4)–Si(7) = 97.33(10), Si(3)–Si(4)–Si(7) = 101.31(10).

solution and were separated under the microscope. For **11** the potassium crown ether unit is coordinating to a SiMe_3 group, whereas in **11a** two potassium crown ether units are coordinating to a cyclopentadienide, thus forming the complex cation we found also frequently in oligosilylated titanocenes in the oxidation state +3.³² For **11a** there are two additional toluene molecules in the asymmetric unit. The comparably small Si–Hf–Si bond angle of 89° for **11** is again diminished compared to a value of 96.4° for the compound with Hf(IV).³⁹ The hafnate **11** features Hf–Si bond distances of 2.85/2.86 Å, which are again elongated in comparison to the neutral Hf(IV) case (2.79/2.83 Å).³⁹ For **11** and **11a** relatively high residual electron density was located close to the Hf atoms.

Compound **14** (Figure 7) crystallizes in the monoclinic space group $P2_1/c$ with one toluene in the asymmetric unit. The structure of the anionic 7-metalla[2.2.1]bicycloheptasilane was already found for the analogous titanocene.³² However, while the titanocene featured the complex cation $[(\text{K} \cdot (18\text{-crown-6}))_2\text{Cp}]^+$, we found for **14** a plain $\text{K} \cdot (18\text{-crown-6})$ moiety which coordinates to a Cp of the metallocene. In comparison to **11** the Hf–Si bonds of **14** are much shorter (2.785/2.790 Å), even shorter than those found for the neutral hafnacyclopentasilane.³⁹ As a consequence of the bicyclic nature of **14** the Si–Hf–Si angle is only 76° .

For compound **14** parts of the geometries of the anionic moieties and some solvent molecules are strongly disordered. Attempts to treat these disorders did not result in diminished residual electron density. As the concerned parts of the structures are not involved in the discussion of structural parameters, it was decided to refrain from the introduction of restraints which would only result in brightened pictures without real improvement of the model.

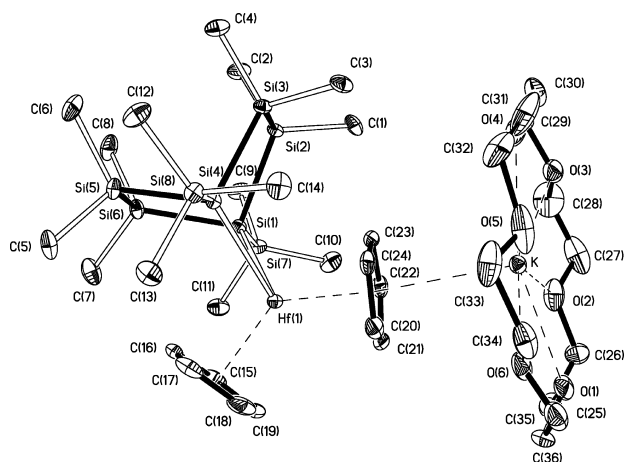


Figure 7. Crystal structure of **14**. Thermal ellipsoids are represented at the probability 30% level, and hydrogen atoms have been omitted for clarity. Selected bond distances (Å) and angles (deg): Hf(1)–Si(1) = 2.785(2), Hf(1)–Si(4) = 2.7900(19), Si(4)–Si(8) = 2.342(3), Si(4)–Si(3) = 2.356(3), Si(4)–Si(5) = 2.357(3), Si(1)–Si(7) = 2.345(3), Si(1)–Si(6) = 2.356(3), Si(1)–Si(2) = 2.363(3), Si(2)–Si(3) = 2.366(3); Si(1)–Hf(1)–Si(4) = 75.98(5), Si(3)–Si(4)–Si(5) = 100.49(11), Si(6)–Si(1)–Si(2) = 100.37(11), Si(1)–Si(2)–Si(3) = 102.19(10), Si(4)–Si(3)–Si(2) = 103.89(10), Si(6)–Si(5)–Si(4) = 102.49(10), Si(5)–Si(6)–Si(1) = 104.06(11).

CONCLUSION

The current study attempts to generalize the chemistry of silylated titanocenes. It was shown that chloride adducts of Cp_2TiCl can simply be obtained by comproportionation of Rosenthal's $\text{Cp}_2\text{Ti}(\text{btmsa})$ with Cp_2TiCl_2 in the presence of either LiCl or KCl and an additional coordinating base (tmeda or 18-crown-6). The lithium or potassium salts of $[\text{Cp}_2\text{TiCl}_2]^-$ thus obtained were used for further reactions with oligosilylanyl dianions. Analogous dichlorinated metalates of zirconium and hafnium could be prepared by reduction of the respective metallocene dichloride with potassium in the presence of 18-crown-6. Also, these metalates could be reacted with oligosilylanyl dianions to give metallacyclopentasilanes with Zr and Hf in a d^1 electron configuration.

In order to gain some insight into the question as to why cyclic dioligosilylated titanocenes seem to be highly unstable and why analogous zircono- and hafnocenocenes are stable only with certain ring sizes, a theoretical study was conducted. The results show that the strong preference for the reductive elimination of disilylated titanocenes is mainly caused by the rather weak Si–Ti bond. The thermodynamic driving force of the reductive elimination of the titanacyclopentasilane in comparison to the analogous Zr and Hf compounds is substantial (171 kJ mol^{-1} (vs Zr) and 199 kJ mol^{-1} (vs Hf)). The reductive elimination to form cyclosilanes is also feasible for zircono- and hafnacyclopentasilanes. However, for these cases the energetic situation is more delicate, as the ring strain in the formed cyclosilanes constitutes a decisive contribution as to whether the reaction is thermodynamically favorable or not.

EPR spectroscopy of a set of d^1 metallacyclopentasilanes was particularly interesting, because these compounds can be regarded either as group 4 d^1 metal complexes or alternatively also as cyclosilylanyl radical anions. While for the d^1 metal the unpaired electron would be considered to be largely localized at the metal, such electrons are considered to be delocalized along the ring atoms in cyclosilylanyl radical anions. A comparison of

the EPR spectra of the Zr(III) compounds **4** and **10** shows that, while no hfs to the attached chlorine atoms in **4** was observed, coupling to the attached silicon atoms indicates delocalization.

EXPERIMENTAL SECTION

General Remarks. All reactions involving air-sensitive compounds were carried out under an atmosphere of dry nitrogen using either Schlenk techniques or a glovebox. All solvents were dried using a column solvent purification system.⁵⁴ Chemicals from different suppliers were used as received without further purification. Elementary analyses were carried out using a Heraeus VARIO ELEMENTAR instrument. EPR spectra were recorded on a Bruker ELEXSYS spectrometer at X-band. Simulation of EPR spectra was done with WinSim2002.⁵⁵

X-ray Structure Determination. For X-ray structure analyses the crystals were mounted onto the tip of glass fibers, and data collection was performed with a Bruker AXS SMART APEX CCD diffractometer using graphite-monochromated Mo $K\alpha$ radiation (0.710 73 Å). The data were reduced to F^2 and corrected for absorption effects with SAINT⁵⁶ and SADABS,^{57,58} respectively. The structures were solved by direct methods and refined by full-matrix least-squares methods (SHELXL97).⁵⁹ If not noted otherwise, all non-hydrogen atoms were refined with anisotropic displacement parameters. All hydrogen atoms were located at calculated positions to correspond to standard bond lengths and angles. All diagrams were drawn with 30% probability thermal ellipsoids, and all hydrogen atoms were omitted for clarity. Crystallographic data (excluding structure factors) for the structures of compounds **3a**, **4**, **7**, **9**, **10**, **11**, **11a**, and **14** reported in this paper have been deposited with the Cambridge Crystallographic Data Center as supplementary publications CCDC 825205 (**3a**), 767184 (**4**), 854110 (**7**), 825206 (**9**), 767185 (**10**), 767187 (**11**), 767189 (**11a**), and 705715 (**14**). Copies of the data can be obtained free of charge at <http://www.ccdc.cam.ac.uk/products/csd/request/>.

Titanocenebis(trimethylsilyl)acetylene,⁶⁰ 1,1-bis(cyclopentadienyl)-2,2,4,4-tetrakis(trimethylsilyl)tetramethylzirconacyclopentasilane (**12**),³⁹ 1,3-dipotassio-1,1,3,3-tetrakis(trimethylsilyl)dimethyltrisilane (**8**),³⁴ 1,4-dipotassio-1,1,4,4-tetrakis(trimethylsilyl)-tetramethyltetrasilane (**1**),³⁴ 1,5-dipotassio-1,1,5,5-tetrakis(trimethylsilyl)hexamethylpentasilane (**6**),³⁴ and 1,4-dipotassio-1,4-bis(trimethylsilyl)octamethylcyclohexasilane (**13**)⁴⁰ were prepared by following published procedures.

General Procedure for the Comproportionation of $\text{Cp}_2\text{Ti}(\text{btmsa})$ with Cp_2TiCl_2 . To a mixture of Cp_2TiCl_2 (249 mg, 1.0 mmol) and $\text{Cp}_2\text{Ti}(\text{btmsa})$ (349 mg, 1.0 mmol) was added THF (5 mL). Immediately a green solution developed, which was stirred for an additional 30 min. All volatiles were removed in vacuo, and the green residue was washed with pentane (2 mL) to yield 426 mg (100%) of $[\text{Cp}_2\text{TiCl}_2]_2$ as a green powder.

The respective alkali-metal chloride adducts could be obtained by adding equimolar amounts of LiCl/tmeda or KCl/18-crown-6 directly to the THF solutions of $[\text{Cp}_2\text{TiCl}_2]_2$ and then following the same workup procedure. Single crystals of blue $\text{Cp}_2\text{TiCl-LiCl}(\text{tmeda})$ (**3a**) were obtained by slow diffusion of pentane into a saturated THF solution. The corresponding $\text{Cp}_2\text{TiCl-KCl}(18\text{-crown-6})$ was crystallized as green crystals from toluene. Anal. Calcd for $\text{C}_{16}\text{H}_{26}\text{Cl}_2\text{LiN}_2\text{Ti}$ (372.101): C, 51.64; H, 7.04; N, 7.53. Found: C, 51.45; H, 6.92; N, 7.23.

General Procedure for the Reduction of Group 4 Metallocene Dichlorides with Potassium/18-crown-6. To a mixture of the respective metallocene dichloride (0.49 mmol), 18-crown-6 (130 mg, 1 equiv), and potassium (19 mg, 1 equiv) was added toluene (5 mL). After 1 h the color started to change and after stirring for 24 h a deeply colored solution was obtained. The reaction mixture was treated with pentane (10 mL), whereupon the product was isolated by filtration.

(18-crown-6)· $\text{K}[\text{Cp}_2\text{ZrCl}_2]$ (**4**) was obtained as an orange crystalline product (286 mg, 98%, mp 117–118 °C). Anal. Calcd for $\text{C}_{22}\text{H}_{34}\text{Cl}_2\text{KO}_6\text{Zr}$ (595.73): C, 44.35; H, 5.75. Found: C, 44.61; H, 5.59. (18-crown-6)· $\text{K}[\text{Cp}_2\text{HfCl}_2]$ (**5**) was obtained as a violet powder

(349 mg, 100%, mp 124–125 °C). Anal. Calcd for $C_{22}H_{34}Cl_2HfKO_6$ (683.00): C, 38.69; H, 5.02. Found: C, 38.47; H, 5.15.

Reactions of Dipotassiooligosilanes 1, 6, and 8 with Titanate 3a. A solution of 1,4-dipotassio-1,1,4,4-tetrakis(trimethylsilyl)tetramethyltetrasilane-(18-crown-6)₂ (**1**; 0.82 mmol) in THF (3 mL) was added to a solution of $[Cp_2TiCl_2][Li(tmeda)]$ (**3a**; 305 mg, 0.82 mmol) in THF (5 mL) at room temperature. Stirring for 3 h was followed by removal of solvent under vacuum. The residue was treated with toluene (5 mL), and the salts were removed by centrifugation. A layer of pentane (8 mL) was placed on the solution, and after 12 h orange-red crystals of **2** (457 mg, 86%) were isolated by decantation.

A solution of 1,5-dipotassio-1,1,5,5-tetrakis(trimethylsilyl)-hexamethylpentasilane-(18-crown-6)₂ (**6**; 0.27 mmol) in THF (4 mL) was added to a solution of $[Cp_2TiCl_2][Li(tmeda)]$ (**3a**; 100 mg, 0.27 mmol) in THF (ca. 2 mL) at room temperature. Stirring for 3 h was followed by addition of pentane (6 mL) to the red solution. After removal of salts and solvent by centrifugation and vacuum the residue was dissolved in toluene (5 mL). A layer of pentane (8 mL) was placed on the solution, and after 16 h red needles of **7** (218 mg) were isolated by decantation.

To a solution of 1,3-dipotassio-1,1,3,3-tetrakis(trimethylsilyl)-dimethyltrisilane-(18-crown-6)₂ (**8**; 0.55 mmol) in toluene (5 mL) was added a solution of $[Cp_2TiCl_2][Li(tmeda)]$ (**3a**; 213 mg, 0.55 mmol) in THF (ca. 5 mL) at –60 °C. Warming to room temperature and stirring for 15 h was followed by addition of pentane (5 mL) to the red solution. After removal of salts by centrifugation crystallization was achieved by cooling to –60 °C for 72 h. Deep red needles of **9** (354 mg, 0.26 mmol, 48%; mp 130–132 °C dec) were obtained.

The identities of **2**, **7**, and **9** were unambiguously established by single-crystal X-ray diffraction analysis.

Reactions of 1,4-Dipotassio-1,1,4,4-tetrakis(trimethylsilyl)-2,2,3,3-tetramethyltetrasilane (1) with 4 and 5. To a stirred solution of 1,4-dipotassio-1,1,4,4-tetrakis(trimethylsilyl)-tetramethyltetrasilane (**1**) in toluene was added dropwise a solution of (18-crown-6)- $K[Cp_2MCl_2]$ ($M = Zr$ (**4**), Hf (**5**)) in toluene (5 mL). Stirring was continued for 3 h, and then half of the solvent was removed under vacuum. The resulting suspension was treated with pentane (0.5 mL), and the obtained precipitate was removed by centrifugation. The deeply colored solution was again treated with pentane (10 mL), and after 24 h crystals of the respective metalate were obtained.

Reaction of **1** (0.43 mmol) with **4** (0.43 mmol) provided orange crystals of **10** (397 mg, mp 127–128 °C). Reaction of **1** (0.51 mmol) with **5** (0.51 mmol) provided a yellow crystalline solid 466 mg) composed of compounds **11** and **11a** (mp of the mixture 164–170 °C). The identities of **10**, **11**, and **11a** were unambiguously established by single-crystal X-ray diffraction analysis.

Reduction of Zirconacyclopentasilane 12 with Potassium in the Presence of 18-crown-6. A mixture of potassium (12 mg, 0.30 mmol), 18-crown-6 (79 mg, 0.30 mmol), and **12** (200 mg, 0.30 mmol) was suspended in toluene (6 mL) and stirred at room temperature for 16 h. The initially red suspension turned into an orange-red solution during this period. The reaction mixture was centrifuged and layered with pentane (ca. 8 mL) to give orange plates after 24 h. The crystals were isolated by decantation and dried under vacuum. Yield: 159 mg (0.12 mmol, 39%). The unambiguous identity of **10** was established by single-crystal X-ray diffraction analysis to be **10a** with the complex cation $[Cp(K-18-crown-6)_2]^+$.

Reaction of 1,4-Dipotassio-1,4-bis(trimethylsilyl)-octamethylcyclohexasilane (13) with Cp_2HfCl_2 . To a solution of 1,4-dipotassio-1,4-bis(trimethylsilyl)octamethylcyclohexasilane (**13**; prepared from 1,1,4,4-tetrakis(trimethylsilyl)-octamethylcyclohexasilane (0.150 mg, 0.258 mmol), 18-crown-6 (140 mg, 2.05 equiv), and KO^tBu (59 mg, 2.05 equiv)) in toluene (5 mL) was added Cp_2HfCl_2 (98 mg, 0.258 mmol) in toluene (3 mL). After 2 h of reaction the formation of 1,4-bis(trimethylsilyl)-dodecamethylbicyclo[2.2.0]octasilane was detected by ^{29}Si NMR spectroscopy.⁴⁰ The formed precipitate was removed by centrifugation, and the solvent was removed under vacuum. The residue was

treated with pentane, and red crystals of **14** were obtained from the solution. The unambiguous identity of **14** was established by single-crystal X-ray diffraction analysis.

■ ASSOCIATED CONTENT

Supporting Information

CIF files, figures, text, and tables giving X-ray crystallographic information for compounds **3a**, **4**, **10**, **11**, and **14** and detailed computational information. This material is available free of charge via the Internet at <http://pubs.acs.org>.

■ AUTHOR INFORMATION

Notes

The authors declare no competing financial interest.

■ ACKNOWLEDGMENTS

This study was supported by the Austrian *Fonds zur Förderung der wissenschaftlichen Forschung* (FWF) via the project P-21346. P.Z. thanks the *Fonds der Chemischen Industrie* (FCI) for a scholarship (No.183191). The Center for Scientific Computing at the CvO University Oldenburg is acknowledged for computer time. We wish to express our gratitude to Ms. Marina Kireenko (Moscow State University) for the translation of ref 24 and to Ms. Tina Konopa for experimental assistance in the early stages of this study.

■ REFERENCES

- (1) *Titanium and Zirconium in Organic Synthesis*; Marek, I., Ed.; Wiley-VCH: Weinheim, Germany, 2002.
- (2) Tilley, T. D. *Acc. Chem. Res.* **1993**, *26*, 22–29.
- (3) Corey, J. Y. *Adv. Organomet. Chem.* **2004**, *51*, 1–52.
- (4) Gauvin, F.; Harrod, J. F.; Woo, H. G. *Adv. Organomet. Chem.* **1998**, *42*, 363–405.
- (5) Reichl, J. A.; Berry, D. H. *Adv. Organomet. Chem.* **1998**, *43*, 197–265.
- (6) Miller, R. D.; Michl, J. *Chem. Rev.* **1989**, *89*, 1359–1410.
- (7) Aitken, C.; Harrod, J. F.; Samuel, E. *J. Organomet. Chem.* **1985**, *279*, C11–C13.
- (8) Aitken, C. T.; Harrod, J. F.; Samuel, E. *J. Am. Chem. Soc.* **1986**, *108*, 4059–4066.
- (9) Harrod, J. F.; Ziegler, T.; Tschinke, V. *Organometallics* **1990**, *9*, 897–902.
- (10) Woo, H. G.; Heyn, R. H.; Tilley, T. D. *J. Am. Chem. Soc.* **1992**, *114*, 5698–5707.
- (11) Harrod, J. F.; Mu, Y.; Samuel, E. *Polyhedron* **1991**, *10*, 1239–1245.
- (12) Hao, L.; Lebus, A.-M.; Harrod, J. F.; Woo, H.-G.; Samuel, E. *Chem. Commun.* **1998**, 2013–2014.
- (13) Samuel, E.; Mu, Y.; Harrod, J. F.; Dromzee, Y.; Jeannin, Y. *J. Am. Chem. Soc.* **1990**, *112*, 3435–3439.
- (14) Hao, L.; Lebus, A.-M.; Harrod, J. F. *Chem. Commun.* **1998**, 1089–1090.
- (15) Hao, L.; Harrod, J. F.; Lebus, A.-M.; Mu, Y.; Shu, R.; Samuel, E.; Woo, H.-G. *Angew. Chem., Int. Ed.* **1998**, *37*, 3126–3129.
- (16) Britten, J.; Mu, Y.; Harrod, J. F.; Polowin, J.; Baird, M. C.; Samuel, E. *Organometallics* **1993**, *12*, 2672–2676.
- (17) Ignatov, S. K.; Rees, N. H.; Tyrrell, B. R.; Dubberley, S. R.; Razuvaev, A. G.; Mountford, P.; Nikonov, G. I. *Chem. Eur. J.* **2004**, *10*, 4991–4999.
- (18) Spaltenstein, E.; Palma, P.; Kreutzer, K. A.; Willoughby, C. A.; Davis, W. M.; Buchwald, S. L. *J. Am. Chem. Soc.* **1994**, *116*, 10308–10309.
- (19) Ohff, A.; Kosse, P.; Baumann, W.; Tillack, A.; Kempe, R.; Goerls, H.; Burlakov, V. V.; Rosenthal, U. *J. Am. Chem. Soc.* **1995**, *117*, 10399–10400.

- (20) Rösch, L.; Altnau, G.; Erb, W.; Pickard, J.; Bruncks, N. *J. Organomet. Chem.* **1980**, *197*, 51–57.
- (21) Holtman, M. S.; Schram, E. P. *J. Organomet. Chem.* **1980**, *187*, 147–155.
- (22) Holtman, M. S.; Schram, E. P. *Inorg. Chim. Acta* **1980**, *41*, 41–47.
- (23) Igonin, V.; Ovchinnikov, Y. E.; Dement'ev, V. V.; Shklover, V. E.; Timofeeva, T. V.; Frunze, T. M.; Struchkov, Y. T. *J. Organomet. Chem.* **1989**, *371*, 187–196.
- (24) Dement'ev, V. V.; Solodovnikov, S. P.; Tumanskii, B. L.; Lavrukhin, B. D.; Frunze, T. M.; Zhdanov, A. A. *Metalloorg. Khim.* **1988**, *1*, 1365–1369.
- (25) Hencken, G.; Weiss, E. *Chem. Ber.* **1973**, *106*, 1747–1751.
- (26) Hao, L.; Lebus, A.-M.; Harrod, J. F.; Hao, L.; Samuel, E. *Chem. Commun.* **1997**, 2193–2194.
- (27) Zirngast, M.; Flock, M.; Baumgartner, J.; Marschner, C. *J. Am. Chem. Soc.* **2009**, *131*, 15952–15962.
- (28) Harrod, J. F.; Malek, A.; Rochon, F. D.; Melanson, R. *Organometallics* **1987**, *6*, 2117–2120.
- (29) Vyshinskaya, L. I.; Vasil'eva, G. A.; Klimova, N. V. *Tr. Khim. Khim. Tekhnol.* **1975**, 79–81.
- (30) Razuvaev, G. A.; Vyshinskaya, L. I.; Vasil'eva, G. A.; Latyaeva, V. N.; Timoshenko, S. Y.; Ermolaev, N. L. *Izv. Akad. Nauk SSSR, Ser. Khim.* **1978**, 2584–2588.
- (31) Razuvaev, G.; Latyaeva, V. N.; Vishinskaya, L. I.; Bytchkov, V. T.; Vasilyeva, G. A. *J. Organomet. Chem.* **1975**, *87*, 93–99.
- (32) Zirngast, M.; Floerke, U.; Baumgartner, J.; Marschner, C. *Chem. Commun.* **2009**, 5538–5540.
- (33) Tamao, K.; Akita, M.; Kanatani, R.; Ishida, N.; Kumada, M. *J. Organomet. Chem.* **1982**, *226*, C9–C13.
- (34) Fischer, R.; Frank, D.; Gaderbauer, W.; Kayser, C.; Mechtler, C.; Baumgartner, J.; Marschner, C. *Organometallics* **2003**, *22*, 3723–3731.
- (35) Coutts, R. S. P.; Wailes, P. C.; Martin, R. L. *J. Organomet. Chem.* **1973**, *47*, 375–382.
- (36) Sekutowski, D. G.; Stucky, G. D. *Inorg. Chem.* **1975**, *14*, 2192–2199.
- (37) Ohff, A.; Pulst, S.; Lefeber, C.; Peulecke, N.; Arndt, P.; Burkalov, V. V.; Rosenthal, U. *Synlett* **1996**, 1996, 111–118.
- (38) Rosenthal, U.; Burlakov, V. V.; Arndt, P.; Baumann, W.; Spannenberg, A. *Organometallics* **2003**, *22*, 884–900.
- (39) Kayser, C.; Kickelbick, G.; Marschner, C. *Angew. Chem., Int. Ed.* **2002**, *41*, 989–992.
- (40) Fischer, R.; Konopa, T.; Ullly, S.; Baumgartner, J.; Marschner, C. *J. Organomet. Chem.* **2003**, *685*, 79–92.
- (41) The Gaussian 09 program was used: *Gaussian 09 Revision B.01*; Gaussian, Inc., Wallingford, CT, 2010.
- (42) For a detailed description of the computations, see the Supporting Information.
- (43) Hehre, W. J.; Ditchfield, R.; Radom, L.; Pople, J. A. *J. Am. Chem. Soc.* **1970**, *92*, 4796–4801.
- (44) Similar strain energies were recently reported for cyclopolysilanes (R₂Si)_n (R = H, i-Pr, n = 3–5): Kudo, T.; Akiba, S.; Kondo, Y.; Watanabe, H.; Morokuma, K.; Vreven, T. *Organometallics* **2003**, *22*, 4721–4724.
- (45) Samuel, E.; Guery, D.; Vedel, J.; Basile, F. *Organometallics* **1985**, *4*, 1073–1077.
- (46) Chatgililoglu, C. *Chem. Rev.* **1995**, *95*, 1229–1251.
- (47) Lacroix, F.; Plecnik, C. E.; Liu, S.; Liu, F.-C.; Meyers, E. A.; Shore, S. G. *J. Organomet. Chem.* **2003**, *687*, 69–77.
- (48) Clearfield, A.; Warner, D. K.; Saldarriaga-Molina, C. H.; Ropal, R.; Bernal, I. *Can. J. Chem.* **1975**, *53*, 1622–1629.
- (49) Gambarotta, S.; Chiang, M. Y. *Organometallics* **1987**, *6*, 897–899.
- (50) Hitchcock, P. B.; Lappert, M. F.; Lawless, G. A.; Olivier, H.; Ryan, E. J. *J. Chem. Soc., Chem. Commun.* **1992**, 474–476.
- (51) Pool, J. A.; Chirik, P. J. *Can. J. Chem.* **2005**, *83*, 286–295.
- (52) Cacciola, J.; Reddy, K. P.; Petersen, J. L. *Organometallics* **1992**, *11*, 665–672.
- (53) Corey, J. Y.; Zhu, X. H.; Brammer, L.; Rath, N. P. *Acta Crystallogr., Sect. C* **1995**, *51*, 565–567.
- (54) Pangborn, A. B.; Giardello, M. A.; Grubbs, R. H.; Rosen, R. K.; Timmers, F. J. *Organometallics* **1996**, *15*, 1518–1520.
- (55) O'Brien, D. A.; Duling, D. R.; Fann, Y. C. *Winsim 2002 (v.0.98)*, *Public EPR Software Tools*; National Institute of Environmental Health Sciences, National Institutes of Health.
- (56) SAINTPLUS: *Software Reference Manual, Version 6.45*; Bruker-AXS: Madison, WI, 1997–2003.
- (57) Sheldrick, G. M. *SADABS, Version 2.10*; Bruker AXS, Madison, WI, 2003.
- (58) Blessing, R. H. *Acta Crystallogr., Sect. A* **1995**, *51*, 33–38.
- (59) Sheldrick, G. M. *Acta Crystallogr., Sect. A* **2007**, *64*, 112–122.
- (60) Burlakov, V. V.; Polyakov, A. V.; Yanovsky, A. I.; Struchkov, Y. T.; Shur, V. B.; Vol'pin, M. E.; Rosenthal, U.; Görls, H. *J. Organomet. Chem.* **1994**, *476*, 197–206.